Deposition of SnS thin films from Sn(II) thioamidate precursors

Amanda L. Catherall, Shasa Harris, Michael S. Hill,* Andrew L. Johnson* and Mary F. Mahon

Department of Chemistry, University of Bath, Claverton Down, Bath, BA2 7AY, UK

Email: msh27@bath.ac.uk; a.l.johnson@bath.ac.uk

Abstract

Introduction

Sunlight is the ultimate source of energy on Earth. Although the photovoltaic (PV) effect remains the most promising means to convert sunlight directly to useable electricity, current devices are dominated by crystalline silicon solar cells. While a mature technology, the indirect band gap of silicon means that the light absorption coefficient is low (102 cm^{-1}) and thick layers (100 – 500 μm) are needed to absorb the requisite number of photons to produce the necessary efficiencies. The cost associated with the production of the thick layers of silicon needed to meet the increasing supply demand is, thus, very high. To date, the supply of sufficient high purity silicon has been economical due to the electronics industry, which produces large amounts of high purity silicon waste. This economic benefit will start to be eroded, however, should the silicon solar sector to continue to grow. To this end, materials containing post-transition metals with an ns^2 electronic configuration (e.g. Pb^{2+}, Sn^{2+}, Ge^{2+}, Sb^{3+} and Bi^{3+}) are attracting significant recent attention for their solar absorber ability.[1] A case in point is provided by tin(II) monosulfide (SnS), which possesses a high absorption coefficient (>104 cm^{-1}) and a near ideal direct band gap of ca. 1.3 eV.[2] Although these properties, in conjunction with the high relative abundance of both tin and sulfur, denote SnS as an attractive candidate photovoltaic absorber, the efficiency of SnS-based devices has yet to reach 5% indicating that significant further advances in materials processing and thin film deposition methods will be required if this promise is to be fulfilled.[3-5]

SnS thin films have been deposited by ALD,[6, 7] spray pyrolysis,[8-13] sputtering,[14-16] chemical bath deposition,[17-29] vacuum evaporation,[30-35] and CVD.[11, 36-49] In this latter regard, an initial report by Price *et al*. described the use of atmospheric pressure (AP) CVD to deposit a variety of tin sulfide stoichiometries from $SnCl_4$ and H_2S in the temperature range 300 – 545 °C,[36, 38] albeit SnS was only obtained at 545 °C. Similarly, (fluoroalkylthiolato)tin(IV) and organotin(IV) dithiocarbamates have been reported to provided SnS under APCVD conditions with the addition of H_2S.[39, 44, 46] The tin thiolate precursor, $(PhS)_4Sn$, has also allowed SnS deposition in the temperature range 350 – 500 ºC both with and without the presence of H_2S by aerosol-assisted (AA) CVD.[40, 41] All the deposited films were amorphous, although Raman spectroscopy and EDX analysis confirmed the presence of tin sulfide. O'Brien and co-workers subsequently described a range of organo tin(IV) and Sn(II) dithiocarbamates, for example the diethyldithiocarbamate derivatives **1** and **2**, which were suitable

for AACVD of orthorhombic α-SnS (Herzenbergite) without a second sulfur source in the temperature range 400 – 530 °C.[48, 50] We have more recently reported that the heteroleptic Sn(II) thioureide compound (**3**) enables AACVD in the temperature range 300 – 450 °C to provide SnS films, the stoichiometry of which was shown by depth profile XPS be consistent with SnS at all successful growth temperatures.[49] Analysis of the photocurrent of the as deposited SnS films was carried out and the external quantum efficiency (EQE) value for α-SnS was calculated to ca. 50%. This value is very high for an untreated and unannealed SnS thin film and demonstrates the clear potential of compounds such as **3** for the successful deposition of SnS PV absorber materials.

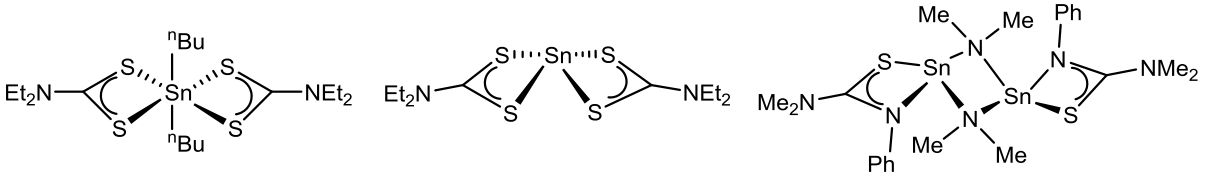

(**1**) (**2**) (**3**)

We have also recently reported that homoleptic Zr(IV) amidates [{RNCR′(O)}$_4$Zr] (R, R′ = alkyl, e.g. *i*-Pr, *t*-Bu) are effective single source precursors for the AACVD of ZrO_x (x = 1.8-1.9).[51] Although the as-deposited films were marginally sub-stoichiometric in oxygen, levels of carbon incorporation were found to be below the XPS detection limit. We reasoned that the viability of such metal amidate derivatives to function as single source precursors to metal oxides is determined by the generalised decomposition pathway shown for an exemplary divalent metal complex in Scheme 1. In this contribution we establish that analogous metal thioamidate derivatives can function as similarly well-defined single source precursors to metal sulfide materials. Specifically, we describe the first reported Sn(II) thioamidates and demonstrate that they have the potential for the AACVD of phase pure SnS, providing excellent control over the Sn(II) oxidation state and at unprecedentedly low temperatures.

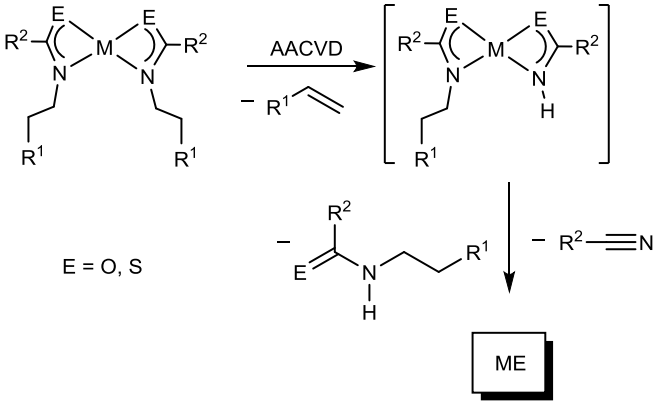

Scheme 1: Proposed decomposition pathway for a metal amidate and thioamidate single source oxide and sulfide precursors under AACVD conditions.

Results and Discussion

The thioamide pro-ligands, L1 and L2, were prepared through reaction of the analogous amides with Lawesson's reagent at 60°C for 18 hours (Scheme 2) and purified by silica gel column

chromatography. The ^{1}H NMR spectra of both pro-ligands displayed a shift in the NH resonance from δ 5.40 ppm in the amides to ca. δ 6.85 ppm in the corresponding thioamide, while the ^{13}C{^{1}H} NMR spectra demonstrated a characteristic shift in the resonance at ca. δ 178 ppm associated with the amide CO double bonds to ca. δ 210 ppm for the C=S double bonds.

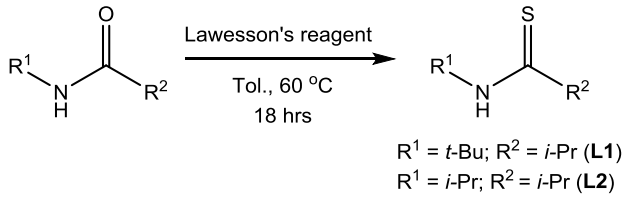

Scheme 2: Reaction scheme for the formation of thioamide ligands L1 and L2.

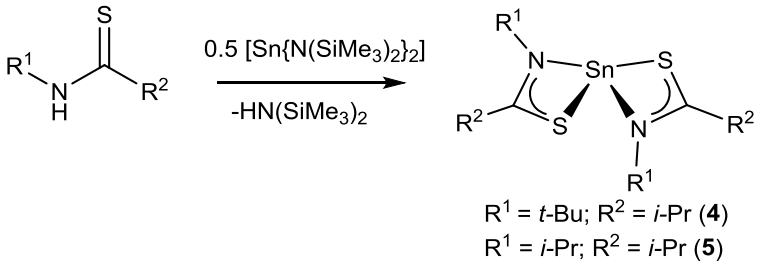

Scheme 3: Synthesis of the Sn(II)thioamidate derivatives **4** and **5**.

The tin(II) thioamidate derivatives, compounds **4** and **5**, were synthesized through the reaction of 0.5 equivalents of [Sn{N(SiMe$_3$)$_2$}$_2$] with L1 and L2 and were isolated as a colorless solid and an orange oil, respectively. The absence of the bis(trimethylsilyl) resonance (ca. 0.29 ppm) in the ^{1}H NMR spectra confirmed that a homoleptic species had been obtained in both compounds, while the appearance of only one set of resonances for the thioamidate ligands in both sets of spectra indicated that the ligands occupy identical environments on the NMR timescale. The ^{119}Sn{^{1}H} NMR spectra for both compounds **4** and **5** were also indicative of a single Sn(II) environment with chemical shifts of δ –318.4 ppm and δ –290.9 ppm, respectively.

X-ray quality single crystals of compound **4** were obtained from a saturated toluene solution at –35 ºC and the resultant structure is shown in Figure 1. Compound **4** exhibits a distorted *pseudo*-square pyramidal geometry, in which the N_2S_2 atoms form the basal plane of the pyramid with the sterochemically active lone pair of the Sn(II) center at the apex. The thioamidate ligands are bound to the Sn(II) atom in a bidentate κ^2-*N*,*S*-fashion and this structure is consistent with the conclusions drawn from the solution NMR analysis of both compounds. The C–S bond length [1.7546(16) Å] is close in value to those reported for typical C-S single bonds whereas the C–N bond [1.2861(18) Å] is more consistent with its assignment as a localised C=N double bond.[44]

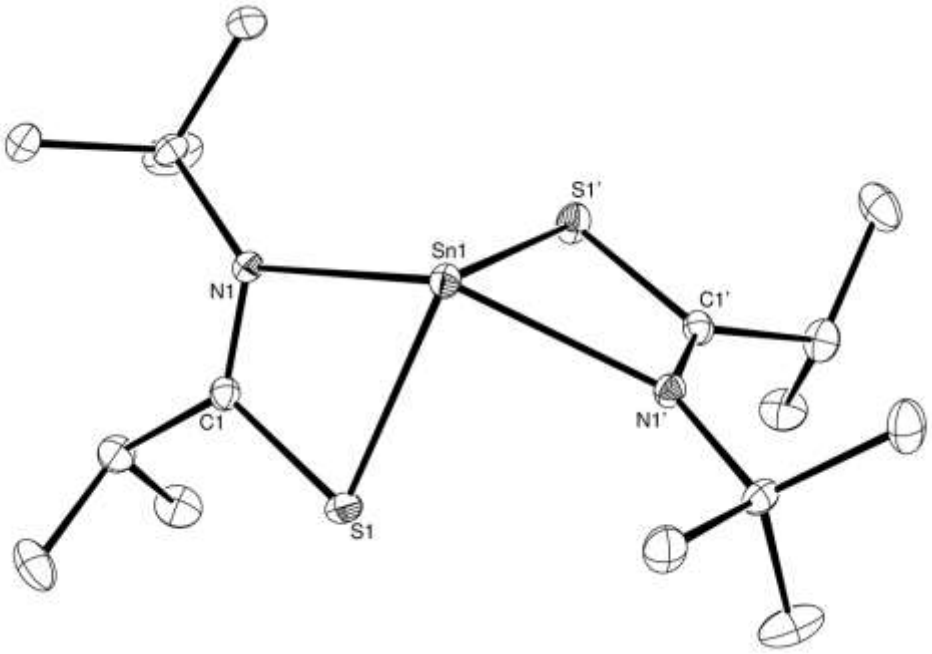

Figure 1: ORTEP representation of compound **4**. Thermal ellipsoids are shown at 25% probability. Atoms with primed labels are related to those in the asymmetric unit by the 1-*x*, 1-*y*, 2-*z* symmetry operation. Selected bond lengths (Å) and angles (°): Sn1-N1 2.3791(12), C1-S1 1.7546(16), Sn1-S1 2.5467(4), C1-N1 1.2861(18), S1-Sn1-S1′, 96.82(2), C1-S1-Sn1 82.24(5), N1′-Sn1-S1 85.95(3), C1-N1-Sn1 99.81(10), N1-Sn1-S1 62.89(3), N1-C1-S1 114.78(11), N1-Sn1-N1′ 133.30(6).

The viability of compounds **4** and **5** to act as potential precursors to SnS was assessed by thermogravimetric analysis (TGA). The resultant thermal decomposition profiles are shown in Figure 2. Compound **4** displays an onset of decomposition at 150 °C and achieves a stable residue accounting for 42 wt% of the initial mass at ca. 300 °C. This residual mass is significantly higher than expected for SnS (34 wt%), which suggests incomplete decomposition and/or the incorporation of non-volatile impurities. In contrast, compound **5** was observed to begin to decompose at ca. 160 ºC and to provide a stable mass residue of 34 wt% at 400 ºC, in close correspondence with that expected for the formation of SnS (36 wt%).

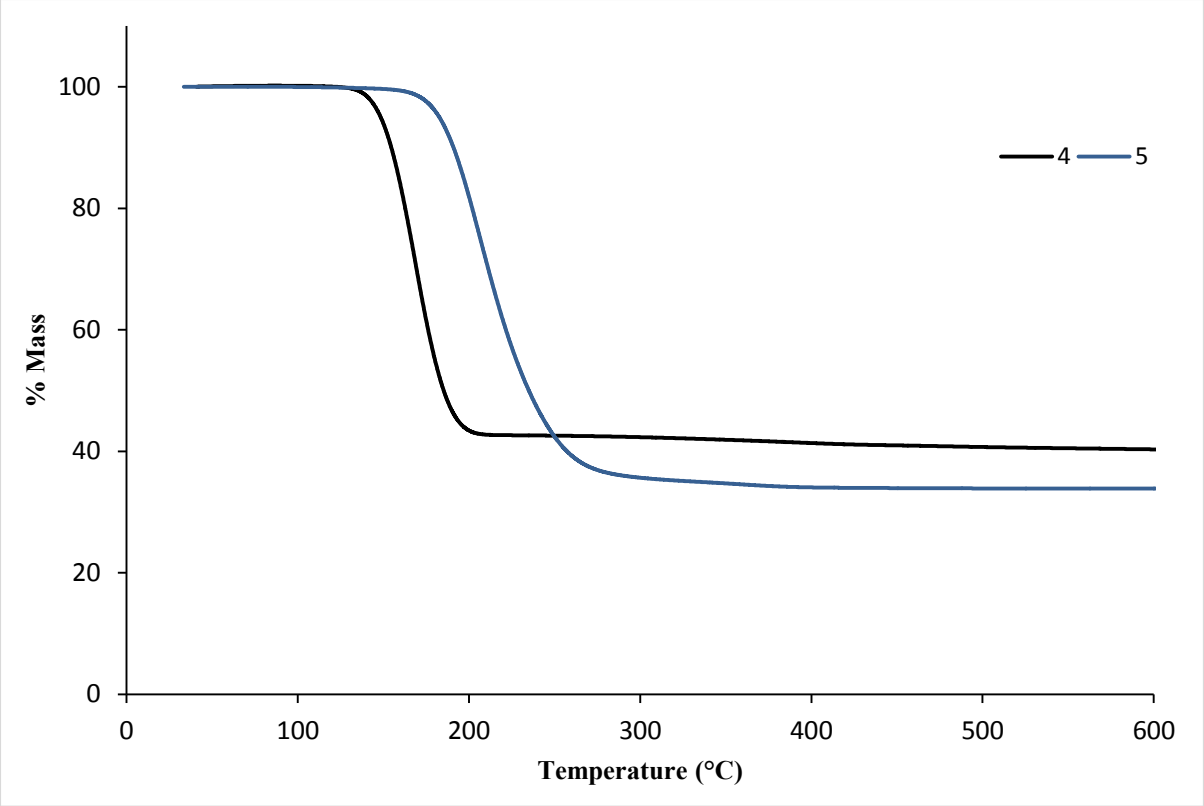

Figure 2: TGA data obtained for compounds **4** and **5**.

The decomposition of both compounds was further studied by analysis of the volatile by-products by ^{1}H NMR spectroscopy. The apparatus was employed as previously described.[51] Guided by the TGA results, compound **4** was heated *in vacuo* at 250 ºC. The resultant ^{1}H NMR spectrum (Figure S1) comprised multiplet signals at δ 4.72 and 1.60 ppm, which were assigned to the respective methylene and methyl environments of 2-methylpropene. The generation of isopropyl nitrile was also confirmed by the observation of heptet and doublet resonances at δ 1.78 and 0.65 ppm. Sublimed solid collected from the cold section of tube located just outside the furnace was also analyzed by ^{1}H NMR spectroscopy. The resultant spectrum allowed the identification of this material as the protonated pro-ligand, L1. The thermal decomposition of compound **5**, performed at 300 ºC (Figure S2), provided similar results, allowing the identification of propylene and isopropyl nitrile as the gaseous products, which were evolved along with sublimed quantities of the pro-ligand L2. We suggest that these results provide strong further support for the generalised mechanism illustrated in Scheme 1 and highlight the potential of both compounds **4** and **5** as molecular precursors to SnS.

Thin Film Deposition

The low onset temperatures of both compounds **4** and **5** (200 °C and 250 °C, respectively), in conjunction with their good solubility in toluene, led us to assess their viability as low temperature single source precursors for AACVD of SnS thin films. The films were deposited under hot wall

conditions in a previously described CVD reactor onto silica-coated float glass substrates (Pilkington NSG Ltd).[51] The deposition conditions are shown in Table 1.

Table 1: Deposition conditions used for the AACVD of SnS thin films with compounds **4** and **5**.

Film	Compound	Concentration (mol dm^{-3})	Temperature (°C)	Deposition time (mins)
A	**4**	0.05	200	30
B	**4**	0.05	250	30
C	**4**	0.05	300	30
D	**5**	0.04	250	30
E	**5**	0.04	300	30
F	**5**	0.05	350	30
G	**5**	0.05	400	30

Photographs of the as-deposited films are shown in Figure S3. Consistent with the inferences drawn from the TGA data, compound **4** typically deposited films at lower temperatures than compound **5** and successful deposition of films **A - C** was achieved with compound **4** in the temperature range 200–300 ºC. The films (**A – C)** were primarily black and opaque in appearance with more visually transparent yellow material at the leading edge of the substrate, which could indicate the presence of SnS and SnS_2 with a clear transition between the two phases. In contrast, compound **5** required higher temperatures (250 – 400 ºC) to effect successful film growth. At the lowest deposition temperature film **D** appeared to be very thin with a brown appearance. Higher temperatures, however, delivered significantly improved coverage of the substrate to provide films which were primarily black in colour. Films **F** and **G** again appeared yellow and transparent at the leading edge of the substrate but with a sharp transition to a continuous black material in a similar manner to the films (**A – B**) deposited from compound **4**. Although the Scotch tape test resulted in the removal of a small quantity of black powder from the surface of the films, the material underneath was found to be opaque, black, continuous and, in some cases, reflective.

Powder X-ray diffraction (pXRD) was performed on all the black regions of the deposited films to determine the crystallinity of the materials. Similar analysis of the yellow regions of the films yielded inconclusive results, presumably as a result of the limited thickness of the material. Representative pXRD patterns for the films deposited from compounds **4** and **5** are shown in Figures

S4 and 3(a) respectively. While film **A**, deposited at 200°C, was found to be amorphous within the limits of the instrument, films **B** and **C** provided one high intensity maximum which could be readily indexed to the (111) reflection of orthorhombic SnS (Card No. 00-014-0620, Herzenbergite). While film **D** was found to be amorphous, films **F** and **G** deposited at the higher temperatures of 350 and 400 °C from compound **5** could also be readily indexed to highly oriented (111) orthorhombic SnS.

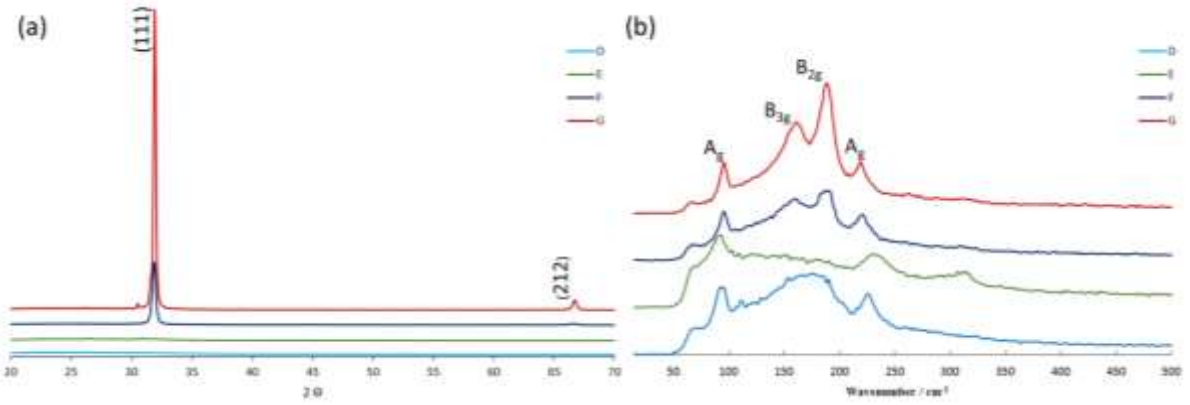

Figure 3: (a) pXRD patterns of films **D** – **G** resulting from AACVD with compound **5**; (b) Raman spectra of films **D** – **G** resulting from AACVD with compound **5**.

The Raman spectra resulting from the black regions of films **A** – **C** (Figure S5) displayed absorptions at 93 (A_g), 158 (B_{3g}), 186 (B_{2g}), 224 cm^{-1} (A_g) and, for **A**, 290 cm^{-1} (B_{2g}). These vibrations correspond with those reported for SnS in the literature,[45, 46, 50] while, significantly, no additional vibrations indicative of the presence of SnS_2, Sn_2S_3 or SnO/SnO_2 could be observed. These data suggest that compound **4** deposits SnS, irrespective of the undetectable level of crystallinity in film **A**, even at the lowest deposition temperature of 200 °C. Films **F** and **G** provided four distinct absorptions at 93, 163, 190, and 220 cm^{-1} (Figure 3(b)), which were similar to those seen in **A** – **C**. Films **D** and **E** also presented Raman data consistent with SnS, however, the spectra were less intense, which we ascribe to the reduction in film thickness as result of the lower temperatures employed. We have previously reported a similar observation related to the SnS films deposited from compound **3** at a deposition temperature of 300 ºC, in which case only peaks of relatively low intensity were observed.[49] In contrast to these observations, film **E** displayed an additional absorption at 312 cm^{-1}, which may be due to the presence of Sn_2S_3 or SnS_2 (Figure 3(b).

XPS analysis was carried out on films **E** – **G** to assess the composition through the thickness of the deposited material. Figure 4(a) shows the depth profile spectra of film **E**. Significantly, the data highlight a Sn:S ratio of ca. 1:1, which would be expected for bulk SnS. Although significant levels of carbon and oxygen were present of the surface of the film, this is attributed to organic contaminants as they reduced dramatically as the sample was etched such that through the bulk of the sample the carbon content was <5 at%. High resolution XPS spectra in the Sn region of the spectrum (Figure

4(b)) comprised the expected $3d_{5/2}$ and $3d_{3/2}$ peaks at binding energies, 486.4 eV and 494.8 eV respectively. Although there is currently some ambiguity with regard to the binding energies of the Sn peaks in SnS,[52] the position of the Sn $3d_{5/2}$ peak for SnS has been reported to typically appear in the range 485.6 – 486.5 eV.[38, 49, 53, 54] Lower intensity peaks at binding energies of 485.2 eV and 493.7 eV are consistent with similar values reported by Mathews *et al.* and are, thus, ascribed to the presence of Sn(0) as Sn metal.[20] The high resolution S spectra displayed the expected doublet $2p_{1/2}$ and $2p_{3/2}$ features at 161.4 and 162.6 eV respectively, consistent with the presence of the S^{2-} anion.[20]

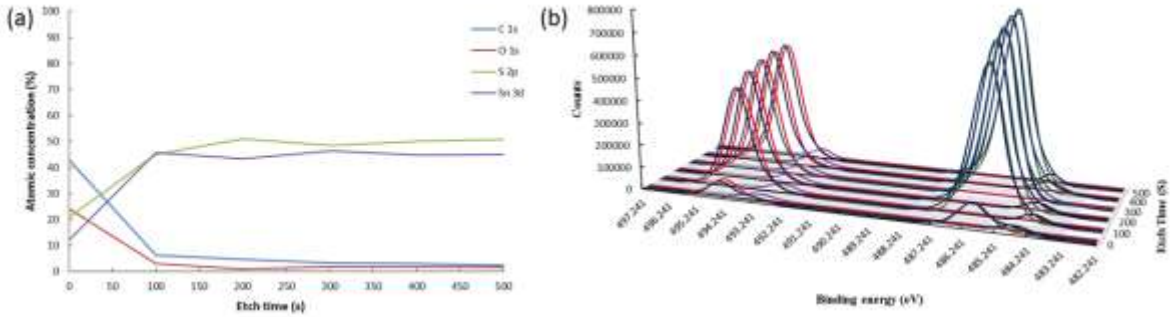

Figure 4: (a) Depth profile XPS data for film **E**; (b) high resolution XPS data for Sn at various etch times for film **E**.

The appearance of silicon and oxygen in the XPS depth profile of film **F** Figure S6), deposited at the higher temperature of 400 °C, were consistent with a reduced film thickness in comparison to that of **E**. As in film **E**, high levels of carbon and oxygen were observed at the surface of the film. The ratio of Sn:S was also found to be rich in Sn, although a ratio of 1:1 appeared close to the interface with the substrate. While the high resolution sulfur spectra displayed the expected doublet feature for S^{2-}, the corresponding Sn spectra highlighted a greater intensity of the 485.2 eV and 493.7 eV emitted photoelectrons, assigned to the presence of elemental tin. While consistent with the Sn:S >1 that was observed through the bulk of the film, we suggest that this observation suggests that the maintenance of the Sn(II) oxidation state provided to the film by precursor **5** begins to be compromised at temperatures >350 °C. Although film **G** was also analysed, the material deposited was found to be too thin, with too much interference from the substrate, to provide a meaningful understanding of the film composition.

Table 2: AFM (rms) roughness values for films **A** – **G**, before and after removal of particulate material.

Film	Temperature (°C)	Roughness before (nm)	Roughness after (nm)
A	200	347	7.6

B	250	558	10.8
C	300	448	136.5
D	250	-	7.6
E	300	-	57.4
F	350	484	43.2
G	400	-	65.2

Atomic force microscopy (AFM) (Figures S7, S8) was performed to determine the root mean square (rms) surface roughness of the SnS thin films, both before and after the removal of the particulate layer (Table 2). Although the rms values of roughness observed for the thin films before the removal of the powder material were very large (> 300 nm), these decreased significantly after it had been removed. In particular, the films deposited at the lowest temperatures (**A**, **B** and **E**) provided roughness values <10 nm, while higher temperatures result in an apparent increase in crystallite size.

These observations were borne out by field emission scanning electron microscopy (FESEM), which was carried out to determine the morphology of the films after the removal of the powder layer. While the plan view of film **B** (Figure 5(a)) illustrates a collection of densely packed large and small plates, the cross-section image (Figure 5(b)) highlights that the film primarily comprises of small crystallites at the surface of the substrate with the larger (ca. 100 nm) plates oriented with an orthogonal disposition to the substrate. In contrast, the image of **C** (Figure 5(c)) illustrates a compact film in which the substrate surface is covered by larger (ca. 300 nm) but more consistently-sized plate-like crystallites. Film **D**, deposited from compound **5**, presents a similar dual morphology (Figure 5(d)), comprising smaller plate-like structures (ca. 430 nm) and some larger features that are more globular in appearance. A general increase in the uniformity of the films is observed with increasing temperature. Consistent with the preferred orientation deduced from the the PXRD patterns of **E** – **F** (Figure 3(a)), the morphology of the films deposited at higher temperatures was dominated by larger platelets (ca. 800 nm) with an approximately perpendicular disposition to the substrate surface (Figures 5(e)). In the case of **F** (Figure 5(f)) there is also evidence of some secondary growth of smaller crystals on the surface of the larger plates.

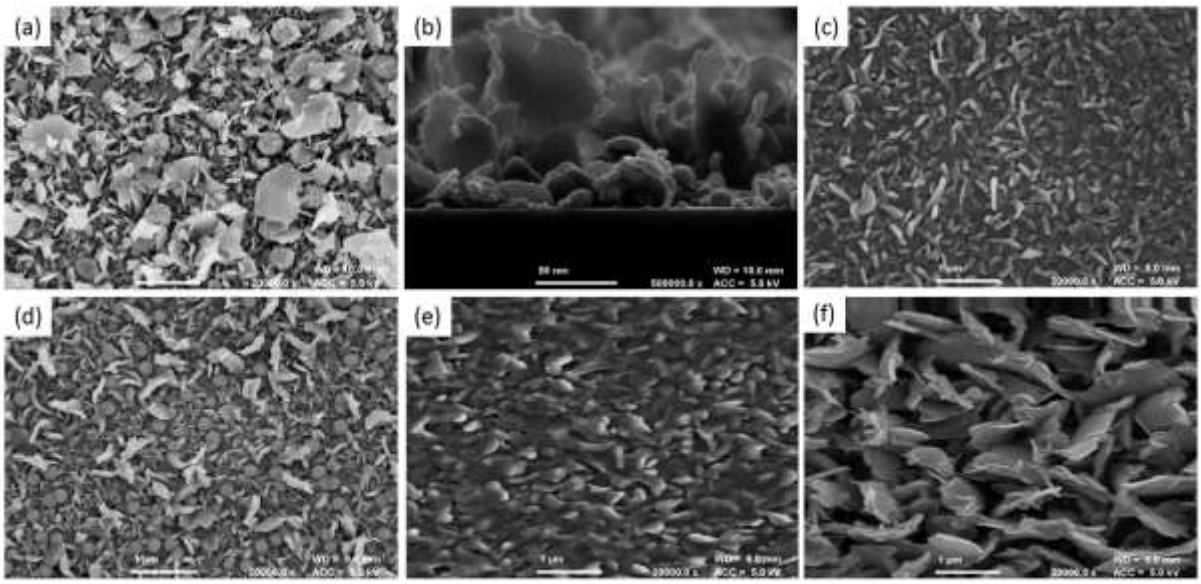

Figure 5: FESEM images (all 20,000× magnification except (b), 50,000×) of AACVD SnS films from compounds **4** and **5**. (a) plan view of film **B**; (b) cross section view of **B**; (c) plan view **C**; (d) plan view **D**; (e) plan view **E**; (f) plan view **F**.

The optical properties of the as-deposited films, **A** – **G** were examined by UV/Vis spectroscopy (Figures S9 and S10) and the construction of the corresponding Tauc plots allowed estimates of the band gap of the films to lie between ca. 1.1 and 1.4 eV, which is consistent with values previously reported for Herzenbergite SnS.[2, 7, 50] Preliminary experiments were also carried out to determine the photocurrent of the as deposited SnS when illuminated under a range of wavelengths. To enable this analysis further films were deposited onto a conducting molybdenum substrate from compound **5** replicating the conditions employed for the growth of films **F** and **G**. Consistent with the observed band gap of the materials, no light was absorbed at wavelengths > ca. 900 nm. Whilst the production of charge carriers remained constant in the visible light region (500 – 800 nm), an observed decrease in the UV region <500 nm may be due to the increased number of recombination of carriers at the surface. The current for the films was extremely small, however, and the resultant EQE value of ca. 0.03 is a factor of a 100 smaller than those values reported for SnS films deposited by AACVD from compound **3**.[49] Although poor absorbers, these preliminary results demonstrate that the films deposited from the Sn(II) amidate precursor **5** produce a current when illuminated by light. Future work will, thus, seek to further optimise the deposition parameters associated with the use of compounds **4** and **5** for the deposition of SnS and these results will be described in future publications.

Experimental

General Techniques. All air and moisture sensitive manipulations were carried out using standard Schlenk line and glovebox techniques under an inert atmosphere of argon. NMR spectra were

collected on a Bruker AV300 spectrometer operating at 300.2 MHz (^{1}H) or 75.5 MHz (^{13}C). The spectra were referenced relative to residual solvent resonances. Solvents (Toluene, THF, hexane) were dried by passage through a commercially available (Innovative Technologies) solvent purification system, under nitrogen and stored in ampoules over molecular sieves. C_6D_6 and d_8-toluene were purchased from Fluorochem Ltd. and dried over molten potassium before distilling under nitrogen and storing over molecular sieves. [Sn{N(SiMe$_3$)$_2$}$_2$] and the amide starting materials were prepared according to literature procedures.[51, 55] TGA data were obtained using a Perkin Elmer TGA 4000 Thermogravimetric Analyzer; analyses were performed air sensitively using samples sealed in crimped aluminum sample pans. Data points were collected every second at a ramp rate of 5°C min^{-1} in a flowing 40 mL min^{-1} N_2 stream. Elemental analyses were performed externally.

General procedure for preparation of thioamide ligands, L1 and L2.

The thioamide ligand precursors were prepared by stirring the relevant amide (1 eq) and commercially available Lawesson's reagent (0.5 eq) together at 60 °C in toluene for 18 hours. Excess Lawesson's reagent was filtered off and the solvent was removed *in vacuo* to afford the product. The product was purified by chromatography column on silica (elution with hexane/ethyl acetate 4:1).

2-methyl-*N*-(2-methyl-2-propanyl)propanthioamide, L1

2-methyl-*N*-(2-methyl-2-propanyl)propanamide (9.46 g, 66.10 mmol) and Lawesson's reagent (13.37 g, 33.10 mmol). Cream oil; further purification carried out using a silica column with hexane:ethyl acetate solvent system at a ratio of 5:1 (9.3 g, 88%). ^{1}H NMR ($CDCl_3$, 300 MHz, 292.0 K) δ (ppm): 7.60 (br. s, N*H*, 1H), 4.53 (m, $^{3}J_{HH}$ = 6.59 Hz, NHC*H*(CH$_3$)$_2$,1H), 2.68 (m, $^{3}J_{HH}$ = 6.78 Hz, C(S)C*H*(CH$_3$)$_2$, 1H), 1.11 (d, NHCH(C*H*$_3$)$_2$, 6H), 1.06 (d, C(S)CH(C*H*$_3$)$_2$, 1H). ^{13}C{^{1}H} NMR ($CDCl_3$, 75 MHz, 293.0 K) δ (ppm): 209.2 (*C*S), 46.5 (NH*C*H(CH$_3$)$_2$), 43.6 (C(S)*C*H(CH$_3$)$_2$), 22.1 (NHCH(**C**H$_3$)$_2$), 20.7 (C(S)CH(*C*H$_3$)$_2$).

N-isopropyl-2-methylpropanthioamide, L2

N-isopropyl-2-methylpropanamide (3.05 g, 28.30 mmol) and Lawesson's reagent (4.71 g, 15.60 mmol). Colourless solid, further purification carried out using a silica column with hexane:ethyl acetate solvent system at a ratio of 4:1 (2.7 g, 60%). ^{1}H NMR ($CDCl_3$, 300 MHz, 292.9 K) δ (ppm): 6.97 (br. s, N*H*, 1H), 2.68 (m, $^{3}J_{HH}$ = 6.78 Hz, C(S)C*H*(CH$_3$)$_2$, 1H), 1.56 (s, NHC(C*H*$_3$)$_3$, 9H), 1.22 (d, C(S)CH(C*H*$_3$)$_2$, 6H). ^{13}C{^{1}H} NMR ($CDCl_3$, 75 MHz, 292.9 K) δ (ppm): 210.2 (*C*S), 55.4 (NH*C*(CH$_3$)$_3$) 46.8 (CS)*C*H(CH$_3$)$_2$), 27.7 (NHCH(*C*H$_3$)$_3$), 22.7 (C(S)CH(*C*H$_3$)$_2$).

General procedure for preparation of tin(II) complexes, 4 and 5.

A solution of [Sn{N(SiMe$_3$)$_2$}$_2$] (1 eq) was added dropwise into a cooled solution of the respective thioamide ligand, L1 or L2 (2 eq). The solution was stirred at the temperature and for the duration stated below for each compound. The solvent was removed *in vacuo* to afford the final product.

Bis(2-methyl-*N*-(1-methylethyl)-propanethioamide)tin(II), 4.

2-methyl-*N*-(2-methyl-2-propanyl)propanthioamide (L1) (1.77 g, 24.5 mmol) and [Sn{N(SiMe$_3$)$_2$}$_2$] (2.68 g, 12.25 mmol) were heated at 60 ºC overnight. Orange oil, no further purification required (0.91 g, 36%). ^{1}H NMR (C$_6$D$_6$, 300 MHz, 291.9 K) δ (ppm): 3.58 (sept., $^3J_{HH}$ = 6.40 Hz, NC*H*(CH$_3$)$_2$, 2H), 2.60 (hept., $^3J_{HH}$ = 6.59 Hz, C(S)C*H*(CH$_3$)$_2$, 2H), 1.08 (d, $^3J_{HH}$ = 6.59, NCH(C*H*$_3$)$_2$, 12H), 1.02 (d, $^3J_{HH}$ = 6.40, C(S)CH(C*H*$_3$)$_2$, 12H). ^{13}C{^{1}H} NMR (C$_6$D$_6$, 75 MHz, 291.9 K) δ (ppm): 193.5 (*C*S), 50.5 (N*C*H(CH$_3$)$_2$) 34.3 (C(S)*C*H(CH$_3$)$_2$), 24.3 (NCH(*C*H$_3$)$_2$), 22.1 (C(S)CH(*C*H$_3$)$_2$). ^{119}Sn NMR (C$_6$D$_6$, 112 MHz, 291.9 K) δ (ppm): −290.9. Elemental analysis: Calculated (found) for C$_{14}$H$_{28}$N$_2$S$_2$Sn: C 41.29 (40.98); H 6.93 (6.76); N 6.88 (6.70)%.

Bis[*N*-(1,1-dimethylethyl)-2-methyl-propanethioamide]tin(II), 5.

N-isopropyl-2-methylpropanthioamide, L2, (1.84 g, 11.50 mmol) and [Sn{N(SiMe$_3$)$_2$}$_2$] (2.52 g, 5.75 mmol) were stirred at room temperature for 1 hour. Peach solid, no further purification required (2.40 g, 96%). Recrystallization was carried out in toluene. ^{1}H NMR (C$_6$D$_6$, 300 MHz, 292.1 K) δ (ppm): 2.78 (m, ^3J_H = 6.59 Hz, C(S)C*H*(CH$_3$)$_2$, 2H), 1.21 (d, C(S)CH(C*H*$_3$)$_2$, 6H), 1.16 (s, NCH(C*H*$_3$)$_3$, 18H), 1.12 (d, C(S)CH(C*H*$_3$)$_2$, 6H). ^{13}C{^{1}H} NMR (C$_6$D$_6$, 75 MHz, 292.1 K) δ (ppm): 195.4 (*C*S), 56.8 (N*C*(CH$_3$)$_3$), 38.3 (C(S)*C*H(CH$_3$)$_2$), 30.1 (NCH(*C*H$_3$)$_3$), 22.1 (C(S)CH(*C*H$_3$)$_2$). ^{119}Sn NMR (C$_6$D$_6$, 112MHz, 292.1K) δ (ppm): −318.4. Elemental analysis: Calculated (found) for C$_{16}$H$_{32}$N$_2$S$_2$Sn: C 44.15 (43.87); H 7.41 (7.28); N 6.44 (6.28)%.

Thermal Decomposition of 4 and 5. In a glovebox a sample of the relevant tin(II) thioamidate (**4** or **5**, *ca.* 0.1 g) was loaded into a silica tube, which was attached to a three way tap. A J Young tap NMR tube charged with 0.5 mL d$_8$-toluene was attached to another outlet of the tap and the whole system was sealed and removed from the glove box. The third outlet of the three way tap was attached to a vacuum line, the NMR tube was cooled to −78°C and the entire apparatus was evacuated (ca 10^{-1} mmHg). At this point the silica tube containing the tin(II) thioamidate was placed inside a Carbolite tube furnace and isolated such that the sample and NMR tubes were connected under a static vacuum while heating.

Compound **4** was heated at 200 °C *in vacuo*. ^{1}H NMR (C$_7$D$_8$, 300 MHz, 294.4 K) δ (ppm): 4.72 (sept., 2H, J_{HH} = 1.13 Hz, C=C*H*$_2$), 1.76 (h, 1H, J_{HH} = 6.97 Hz, C*H*), 1.60 (d, 6H, J_{HH} = 1.13 Hz, C*H*$_3$), 0.49 (d, 6H, J_{HH} = 6.97 Hz, C*H*$_3$). ^{13}C{^{1}H} NMR (C$_7$D$_8$, 75 MHz, 294.5 K) δ (ppm): 141.8 (H$_2$C=*C*), 111.1 (H$_2$*C*=C), 24.0 (*C*H$_3$), 19.6 (*C*H(CH$_3$)$_2$), 19.5 (CH(*C*H$_3$)$_2$).

Compound **5** was heated at 300 °C *in vacuo*. ^{1}H NMR (C_7D_8, 300 MHz, 294.4 K) δ (ppm): 5.71 (m, 1H, H_2C=C*H*), 4.96 (m, 2H, *H*$_2$C=CH), 1.75 (h, 1H, J_{HH} = 6.97 Hz, C*H*), 1.56 (dt, 3H, C*H*$_3$), 0.63 (d, 6H, J_{HH} = 6.97 Hz, C*H*$_3$). The sample was too weak for the acquisition of meaningful ^{13}C NMR data.

X-ray Crystallography

Single crystals of compound **4** were isolated from toluene solution at −35 °C. A suitable crystal was selected and on a Xcalibur EosS2 diffractometer. The crystal was kept at 173.15 K during data collection. Using Olex2,[56] the structure was solved with the olex2.solve[57] structure solution program using Charge Flipping and refined with the ShelXL refinement package using Least Squares minimisation.[58] The asymmetric unit of **4** comprised ½ of a molecule of the tin complex, with the central metal atom lying on a special position (2-fold rotation axis) available in this space group and a small amount of disordered solvent. The latter equates to ½ of a molecule of toluene in the asymmetric unit and this allowance has been included in the formula – although the solvent was ultimately treated with the PLATON SQUEEZE algorithm.

Crystal Data for $C_{11.5}H_{20}NSSn_{0.5}$ (*M* =263.69 g/mol): monoclinic, space group *C*2/*c* (no. 15), *a* = 14.9328(5) Å, *b* = 11.1960(3) Å, *c* = 16.3662(5) Å, *β* = 102.642(3)°, *V* = 2669.90(14) Å^3, *Z* = 8, *μ*(Mo K*α*) = 1.124 mm^{-1}, *Dcalc* = 1.312 g/cm^3, 10461 reflections measured (6.696° ≤ 2Θ ≤ 54.93°), 3009 unique (R_{int} = 0.0282, R_{sigma} = 0.0306) which were used in all calculations. The final R_1 was 0.0203 (I > 2*σ*(I)) and wR_2 was 0.0438 (all data).

Acknowledgements

We thank the University of Bath for funding of a PhD studentship (ALC) and a MChem project (SH).

References

(1) Ganose, A. M.; Savory, C. N.; Scanlon, D. O., Beyond methylammonium lead iodide: prospects for the emergent field of ns(2) containing solar absorbers. *Chemical Communications* **2017,** 53, (1), 20-44.
(2) Tanusevski, A.; Poelman, D., Optical and photoconductive properties of SnS thin films prepared by electron beam evaporation. *Solar Energy Materials and Solar Cells* **2003,** 80, (3), 297-303.
(3) Sinsermsuksakul, P.; Sun, L. Z.; Lee, S. W.; Park, H. H.; Kim, S. B.; Yang, C. X.; Gordon, R. G., Overcoming Efficiency Limitations of SnS-Based Solar Cells. *Advanced Energy Materials* **2014,** 4, (15).
(4) Banai, R. E.; Horn, M. W.; Brownson, J. R. S., A review of tin (II) monosulfide and its potential as a photovoltaic absorber. *Solar Energy Materials and Solar Cells* **2016,** 150, 112-129.
(5) Burton, L. A.; Kumagai, Y.; Walsh, A.; Oba, F., DFT investigation into the underperformance of sulfide materials in photovoltaic applications. *Journal of Materials Chemistry A* **2017,** 5, (19), 9132-9140.
(6) Kim, J. Y.; George, S. M., Tin Monosulfide Thin Films Grown by Atomic Layer Deposition Using Tin 2,4-Pentanedionate and Hydrogen Sulfide. *Journal of Physical Chemistry C* **2010,** 114, (41), 17597-17603.
(7) Sinsermsuksakul, P.; Heo, J.; Noh, W.; Hock, A. S.; Gordon, R. G., Atomic Layer Deposition of Tin Monosulfide Thin Films. *Advanced Energy Materials* **2011,** 1, (6), 1116-1125.

(8) Reddy, K. T. R.; Reddy, P. P.; Miles, R. W.; Datta, P. K., Investigations on SnS films deposited by spray pyrolysis. *Optical Materials* **2001,** 17, (1-2), 295-298.
(9) Reddy, K. T. R.; Reddy, P. P.; Datta, R.; Miles, R. W., Formation of polycrystalline SnS layers by a two-step process. *Thin Solid Films* **2002,** 403, 116-119.
(10) Thangaraju, B.; Kaliannan, P., Spray pyrolytic deposition and characterization of SnS and SnS2 thin films. *Journal of Physics D-Applied Physics* **2000,** 33, (9), 1054-1059.
(11) Calixto-Rodriguez, M.; Martinez, H.; Sanchez-Juarez, A.; Campos-Alvarez, J.; Tiburcio-Silver, A.; Calixto, M. E., Structural, optical, and electrical properties of tin sulfide thin films grown by spray pyrolysis. *Thin Solid Films* **2009,** 517, (7), 2497-2499.
(12) Boudjouk, P.; Seidler, D. J.; Grier, D.; McCarthy, G. J., Benzyl-substituted tin chalcogenides. Efficient single-source precursors for tin sulfide, tin selenide, and Sn(SxSe1-x) solid solutions. *Chemistry of Materials* **1996,** 8, (6), 1189-1196.
(13) Reddy, K. T. R.; Reddy, N. K.; Miles, R. W., Photovoltaic properties of SnS based solar cells. *Solar Energy Materials and Solar Cells* **2006,** 90, (18-19), 3041-3046.
(14) Xu, J. X.; Yang, Y. Z.; Xie, Z. W., Fabrications of SnS thin films and SnS-based heterojunctions on flexible polyimide substrates. *Journal of Materials Science-Materials in Electronics* **2014,** 25, (7), 3028-3033.
(15) Ghosh, B.; Das, M.; Banerjee, R.; Das, S., Fabrication of vacuum-evaporated SnS/CdS heterojunction for PV applications. *Solar Energy Materials and Solar Cells* **2008,** 92, (9), 1099-1104.
(16) Reddy, V. R. M.; Gedi, S.; Park, C.; Miles, R. W.; Reddy, K. T. R., Development of sulphurized SnS thin film solar cells. *Current Applied Physics* **2015,** 15, (5), 588-598.
(17) Avellaneda, D.; Delgado, G.; Nair, M. T. S.; Nair, P. K., Structural and chemical transformations in SnS thin films used in chemically deposited photovoltaic cells. *Thin Solid Films* **2007,** 515, (15), 5771-5776.
(18) Avellaneda, D.; Nair, M. T. S.; Nair, P. K., Polymorphic tin sulfide thin films of zinc blende and orthorhombic structures by chemical deposition. *Journal of the Electrochemical Society* **2008,** 155, (7), D517-D525.
(19) Avellaneda, D.; Nair, M. T. S.; Nair, P. K., Photovoltaic structures using chemically deposited tin sulfide thin films. *Thin Solid Films* **2009,** 517, (7), 2500-2502.
(20) Mathews, N. R.; Avellaneda, D.; Anaya, H. B. M.; Campos, J.; Nair, M. T. S.; Nair, P. K.; Mrs In *Chemically and electrochemically deposited thin films of tin sulfide for photovoltaic structures*, Symposium on Thin-Film Compound Semiconductor Photovoltaics, San Francisco, CA, Apr 13-17, 2009; San Francisco, CA, 2009; pp 367-+.
(21) Hankare, P. P.; Jadhav, A. V.; Chate, P. A.; Rathod, K. C.; Chavan, P. A.; Ingole, S. A., Synthesis and characterization of tin sulphide thin films grown by chemical bath deposition technique. *Journal of Alloys and Compounds* **2008,** 463, (1-2), 581-584.
(22) Turan, E.; Kul, M.; Aybek, A. S.; Zor, M., Structural and optical properties of SnS semiconductor films produced by chemical bath deposition. *Journal of Physics D-Applied Physics* **2009,** 42, (24).
(23) Akkari, A.; Guasch, C.; Kamoun-Turki, N., Chemically deposited tin sulphide. *Journal of Alloys and Compounds* **2010,** 490, (1-2), 180-183.
(24) Guneri, E.; Gode, F.; Ulutas, C.; Kirmizigul, F.; Altindemir, G.; Gumus, C., PROPERTIES OF P-TYPE SnS THIN FILMS PREPARED BY CHEMICAL BATH DEPOSITION. *Chalcogenide Letters* **2010,** 7, (12), 685-694.
(25) Guneri, E.; Ulutas, C.; Kirmizigul, F.; Altindemir, G.; Gode, F.; Gumus, C., Effect of deposition time on structural, electrical, and optical properties of SnS thin films deposited by chemical bath deposition. *Applied Surface Science* **2010,** 257, (4), 1189-1195.
(26) Reghima, M.; Akkari, A.; Guasch, C.; Turki-Kamoun, N., Structure, Surface Morphology, and Optical and Electronic Properties of Annealed SnS Thin Films Obtained by CBD. *Journal of Electronic Materials* **2014,** 43, (9), 3138-3144.
(27) Gao, C.; Shen, H. L., Influence of the deposition parameters on the properties of orthorhombic SnS films by chemical bath deposition. *Thin Solid Films* **2012,** 520, (9), 3523-3527.
(28) Gedi, S.; Reddy, V. R. M.; Park, C.; Chan-Wook, J.; Reddy, K. T. R., Comprehensive optical studies on SnS layers synthesized by chemical bath deposition. *Optical Materials* **2015,** 42, 468-475.

(29) Reddy, N. K.; Devika, M.; Ahsanulhaq, Q.; Gunasekhar, K. R., Growth of Orthorhombic SnS Nanobox Structures on Seeded Substrates. *Crystal Growth & Design* **2010,** 10, (11), 4769-4772.
(30) Devika, M.; Reddy, K. T. R.; Reddy, N. K.; Ramesh, K.; Ganesan, R.; Gopal, E. S. R.; Gunasekhar, K. R., Microstructure dependent physical properties of evaporated tin sulfide films. *Journal of Applied Physics* **2006,** 100, (2).
(31) Reddy, N. K.; Ramesh, K.; Ganesan, R.; Reddy, K. T. R.; Gunasekhar, K. R.; Gopal, E. S. R., Synthesis and characterisation of co-evaporated tin sulphide thin films. *Applied Physics a-Materials Science & Processing* **2006,** 83, (1), 133-138.
(32) Devika, M.; Reddy, N. K.; Ramesh, K.; Ganesan, R.; Gunasekhar, K. R.; Gopal, E. S. R.; Reddy, K. T. R., Thickness effect on the physical properties of evaporated SnS films. *Journal of the Electrochemical Society* **2007,** 154, (2), H67-H73.
(33) Steinmann, V.; Jaramillo, R.; Hartman, K.; Chakraborty, R.; Brandt, R. E.; Poindexter, J. R.; Lee, Y. S.; Sun, L. Z.; Polizzotti, A.; Park, H. H.; Gordon, R. G.; Buonassisi, T., 3.88% Efficient Tin Sulfide Solar Cells using Congruent Thermal Evaporation. *Advanced Materials* **2014,** 26, (44), 7488-7492.
(34) Jaramillo, R.; Steinmann, V.; Yang, C. X.; Hartman, K.; Chakraborty, R.; Poindexter, J. R.; Castillo, M. L.; Gordon, R.; Buonassisi, T., Making Record-efficiency SnS Solar Cells by Thermal Evaporation and Atomic Layer Deposition. *Jove-Journal of Visualized Experiments* **2015**, (99).
(35) Schneikart, A.; Schimper, H. J.; Klein, A.; Jaegermann, W., Efficiency limitations of thermally evaporated thin-film SnS solar cells. *Journal of Physics D-Applied Physics* **2013,** 46, (30).
(36) Price, L. S.; Parkin, I. P.; Hibbert, T. G.; Molloy, K. C., Atmospheric pressure CVD of SnS and SnS2 on glass. *Chemical Vapor Deposition* **1998,** 4, (6), 222-+.
(37) Parkin, I. P.; Price, L. S.; Hardy, A. M. E.; Clark, R. J. H.; Hibbert, T. G.; Molloy, K. C., Atmospheric pressure chemical vapour deposition of tin sulfide thin films. *Journal De Physique Iv* **1999,** 9, (P8), 403-410.
(38) Price, L. S.; Parkin, I. P.; Hardy, A. M. E.; Clark, R. J. H.; Hibbert, T. G.; Molloy, K. C., Atmospheric pressure chemical vapor deposition of tin sulfides (SnS, Sn2S3, and SnS2) on glass. *Chemistry of Materials* **1999,** 11, (7), 1792-1799.
(39) Price, L. S.; Parkin, I. P.; Field, M. N.; Hardy, A. M. E.; Clark, R. J. H.; Hibbert, T. G.; Molloy, K. C., Atmospheric pressure chemical vapour deposition of tin(II) sulfide films on glass substrates from (Bu3SnO2CCF3)-Sn-n with hydrogen sulfide. *Journal of Materials Chemistry* **2000,** 10, (2), 527-530.
(40) Barone, G.; Hibbert, T. G.; Mahon, M. F.; Molloy, K. C.; Price, L. S.; Parkin, I. P.; Hardy, A. M. E.; Field, M. N., Deposition of tin sulfide thin films from tin(IV) thiolate precursors. *Journal of Materials Chemistry* **2001,** 11, (2), 464-468.
(41) Barone, G.; Hibbert, T.; Mahon, M. F.; Molloy, K. C.; Parkin, I. P.; Price, L. S.; Silaghi-Dumitrescu, I., Structural distortions in homoleptic (RE)(4)A (E = O, S, Se; A = C, Si, Ge, Sn): implications for the CVD of tin sulfides. *Journal of the Chemical Society-Dalton Transactions* **2001**, (23), 3435-3445.
(42) Hibbert, T. G.; Kana, A. T.; Mahon, M. F.; Molloy, K. C.; Price, L. S.; Parkin, I. P.; Venter, M. M., Designing precursors for the deposition of tin sulphide thin films. *Main Group Metal Chemistry* **2001,** 24, (9), 633-636.
(43) Hibbert, T. G.; Mahon, M. F.; Molloy, K. C.; Price, L. S.; Parkin, I. P., Deposition of tin sulfide thin films from novel, volatile (fluoroalkythiolato)tin(IV) precursors. *Journal of Materials Chemistry* **2001,** 11, (2), 469-473.
(44) Kana, A. T.; Hibbert, T. G.; Mahon, M. F.; Molloy, K. C.; Parkin, I. P.; Price, L. S., Organotin unsymmetric dithiocarbamates: synthesis, formation and characterisation of tin(II) sulfide films by atmospheric pressure chemical vapour deposition. *Polyhedron* **2001,** 20, (24-25), 2989-2995.
(45) Parkin, I. P.; Price, L. S.; Hibbert, T. G.; Molloy, K. C., The first single source deposition of tin sulfide coatings on glass: aerosol-assisted chemical vapour deposition using Sn(SCH2CH2S)(2). *Journal of Materials Chemistry* **2001,** 11, (5), 1486-1490.
(46) Barone, G.; Chaplin, T.; Hibbert, T. G.; Kana, A. T.; Mahon, M. F.; Molloy, K. C.; Worsley, I. D.; Parkin, I. P.; Price, L. S., Synthesis and thermal decomposition studies of homo- and heteroleptic tin(IV) thiolates and dithiocarbamates: molecular precursors for tin sulfides. *Journal of the Chemical Society-Dalton Transactions* **2002**, (6), 1085-1092.

(47) Bade, B. P.; Garje, S. S.; Niwate, Y. S.; Afzaal, M.; O'Brien, P., Tribenzyltin(IV) chloride Thiosemicarbazones: Novel Single Source Precursors for Growth of SnS Thin Films. *Chemical Vapor Deposition* **2008,** 14, (9-10), 292-295.
(48) Kevin, P.; Lewis, D. J.; Raftery, J.; Malik, M. A.; O'Brien, P., Thin films of tin(II) sulphide (SnS) by aerosol-assisted chemical vapour deposition (AACVD) using tin(II) dithiocarbamates as single-source precursors. *Journal of Crystal Growth* **2015,** 415, 93-99.
(49) Ahmet, I. Y.; Hill, M. S.; Johnson, A. L.; Peter, L. M., Polymorph-Selective Deposition of High Purity SnS Thin Films from a Single Source Precursor. *Chemistry of Materials* **2015,** 27, (22), 7680-7688.
(50) Ramasamy, K.; Kuznetsov, V. L.; Gopal, K.; Malik, M. A.; Raftery, J.; Edwards, P. P.; O'Brien, P., Organotin Dithiocarbamates: Single-Source Precursors for Tin Sulfide Thin Films by Aerosol-Assisted Chemical Vapor Deposition (AACVD). *Chemistry of Materials* **2013,** 25, (3), 266-276.
(51) Catherall, A. L.; Hill, M. S.; Johnson, A. L.; Kociok-Kohn, G.; Mahon, M. F., Homoleptic zirconium amidates: single source precursors for the aerosol-assisted chemical vapour deposition of ZrO2. *Journal of Materials Chemistry C* **2016,** 4, (45), 10731-10739.
(52) Whittles, T. J.; Burton, L. A.; Skelton, J. M.; Walsh, A.; Veal, T. D.; Dhanak, V. R., Band Alignments, Valence Bands, and Core Levels in the Tin Sulfides SnS, SnS2, and Sn2S3: Experiment and Theory. *Chemistry of Materials* **2016,** 28, (11), 3718-3726.
(53) Balaz, P.; Ohtani, T.; Bastl, Z.; Boldizarova, E., Properties and reactivity of mechanochemically synthesized tin sulfides. *Journal of Solid State Chemistry* **1999,** 144, (1), 1-7.
(54) Cruz, M.; Morales, J.; Espinos, J. P.; Sanz, J., XRD, XPS and Sn-119 NMR study of tin sulfides obtained by using chemical vapor transport methods. *Journal of Solid State Chemistry* **2003,** 175, (2), 359-365.
(55) Fjeldberg, T.; Hope, H.; Lappert, M. F.; Power, P. P.; Thorne, A. J., MOLECULAR-STRUCTURES OF THE MAIN GROUP 4 METAL(II) BIS(TRIMETHYLSILYL)-AMIDES M N(SIME3)2 2 IN THE CRYSTAL (X-RAY) AND VAPOR (GAS-PHASE ELECTRON-DIFFRACTION). *Journal of the Chemical Society-Chemical Communications* **1983**, (11), 639-641.
(56) Dolomanov, O. V.; Bourhis, L. J.; Gildea, R. J.; Howard, J. A. K.; Puschmann, H., OLEX2: a complete structure solution, refinement and analysis program. *Journal of Applied Crystallography* **2009,** 42, 339-341.
(57) Bourhis, L. J.; Dolomanov, O. V.; Gildea, R. J.; Howard, J. A. K.; Puschmann, H., The anatomy of a comprehensive constrained, restrained refinement program for the modern computing environment-Olex2 dissected. *Acta Crystallographica a-Foundation and Advances* **2015,** 71, 59-75.
(58) Sheldrick, G. M., Crystal structure refinement with SHELXL. *Acta Crystallographica Section C-Structural Chemistry* **2015,** 71, 3-8.